Check for updates

Geophysical Research Letters

RESEARCH LETTER
10.1029/2022GL099324

Key Points:

- For the mountainous catchments in the Upper Colorado River, the fate of snow (rain) is 33% (67%) evapotranspiration (ET) and 13% (8%) summer streamflow
- In catchments with relatively higher tree cover, snow was more likely to evapotranspire with less rain and snow sustaining streamflow
- Increased rainfall led to greater share of rain in ET rather than streamflow, while snowfall variation had little effect

Supporting Information:

Supporting Information may be found in the online version of this article.

Correspondence to:

M. Sprenger,
msprenger@lbl.gov

Citation:

Sprenger, M., Carroll, R. W. H., Dennedy-Frank, J., Siirila-Woodburn, E. R., Newcomer, M. E., Brown, W., et al. (2022). Variability of snow and rainfall partitioning into evapotranspiration and summer runoff across nine mountainous catchments. *Geophysical Research Letters*, *49*, e2022GL099324. https://doi.org/10.1029/2022GL099324

Received 28 APR 2022
Accepted 22 JUN 2022

Author Contributions:

Conceptualization: Matthias Sprenger
Data curation: Rosemary W. H. Carroll, Michelle E. Newcomer, Wendy Brown, Alexander Newman, Curtis Beutler, Markus Bill, Kenneth H. Williams
Formal analysis: Matthias Sprenger

© 2022 The Authors. This article has been contributed to by U.S. Government employees and their work is in the public domain in the USA.
This is an open access article under the terms of the Creative Commons Attribution-NonCommercial-NoDerivs License, which permits use and distribution in any medium, provided the original work is properly cited, the use is non-commercial and no modifications or adaptations are made.

Variability of Snow and Rainfall Partitioning Into Evapotranspiration and Summer Runoff Across Nine Mountainous Catchments

Matthias Sprenger[1], Rosemary W. H. Carroll[2], James Dennedy-Frank[1], Erica R. Siirila-Woodburn[1], Michelle E. Newcomer[1], Wendy Brown[3], Alexander Newman[3], Curtis Beutler[3], Markus Bill[1], Susan S. Hubbard[4], and Kenneth H. Williams[1,3]

[1]Lawrence Berkeley National Laboratory, Berkeley, CA, USA, [2]Desert Research Institute, Reno, NV, USA, [3]Rocky Mountain Biological Laboratory, Crested Butte, CO, USA, [4]Oak Ridge National Laboratory, Oak Ridge, TN, USA

Abstract Understanding the partitioning of snow and rain contributing to either catchment streamflow or evapotranspiration (ET) is of critical relevance for water management in response to climate change. To investigate this partitioning, we use endmember splitting and mixing analyses based on stable isotope (^{18}O) data from nine headwater catchments in the East River, Colorado. Our results show that one third of the snow partitions to ET and 13% of the snowmelt sustains summer streamflow. Only 8% of the rainfall contributes to the summer streamflow, because most of the rain (67%) partitions to ET. The spatial variability of precipitation partitioning is mainly driven by aspect and tree cover across the sub-catchments. Catchments with higher tree cover have a higher share of snow becoming ET, resulting in less snow in summer streamflow. Summer streamflow did not contain more rain with higher rainfall sums, but more rain was taken up in ET.

Plain Language Summary Snowmelt from the Rocky Mountains is crucial for the water supply in the Upper Colorado River Basin (UCRB). With reduced snowpack and earlier snowmelt due to climate change, it is important to understand how much of the snow directly contributes to streamflow and how much returns directly to the atmosphere via evaporation and vegetation use, called evapotranspiration (ET). We applied a stable isotope mass balance approach to investigate this for nine catchments in the UCRB. We found that snow sustains not only most the streamflow but also ¾ of the ET. Rainfall was mostly (2/3) lost to the atmosphere through ET. The variation of the snow and rain contributions to streamflow and ET were mainly driven by the catchment aspect and tree cover. The findings show that the timing of snowmelt (influenced by aspect) and plant water use (influenced by tree cover) determined how much snow became streamflow and ET.

1. Introduction

Mountainous systems are among the most sensitive environments to a warming climate because of shifts that occur when snowfall is reduced and snowmelt takes place earlier due to higher temperatures (Hock et al., 2019). Such changes are already observed (e.g., Musselman et al., 2021) and have been further projected (e.g., Ikeda et al., 2021) for the Rocky Mountains. It is crucial to understand how snow and rain impact the runoff (Q) and evapotranspiration (ET) dynamics because of their role in sustaining the water supply in downstream regions (Immerzeel et al., 2020). Inter-seasonal storage transfer is an important process that needs to be well understood to account for its potential impacts on ecosystem and anthropogenic water supply due to the interplay of a highly seasonal water input during snowmelt, the resulting hydrograph peak, and the strong seasonality of ET fluxes. Disentangling how snow and rain partition into Q and ET is critical for understanding potential ramifications of a low-snow to no-snow future (Woodburn et al., 2021).

While snow is recognized as a key source for the water supply in the Western US (Li et al., 2017), the relative share of snow versus rain in sustaining vegetation (i.e., ET) and the relative fraction of snow and rain becoming Q and ET remains currently unclear. Tracer approaches which can track the fate of rain and snow in mountainous hydrological systems can fill this gap. A strong difference in the stable isotope ratios (^{2}H and ^{18}O) of snowfall and rainfall enables isotope-based endmember mixing and splitting analyses (Kirchner & Allen, 2020) to derive the relative share of these inputs in the Q and ET fluxes (i.e., "mixing"), as well as partitioning of the inputs into Q and ET (i.e., "splitting"). Here, we apply such isotope mass balance analyses for nine headwater catchments

Investigation: Matthias Sprenger, Rosemary W. H. Carroll, James Dennedy-Frank, Erica R. Siirila-Woodburn, Wendy Brown, Alexander Newman, Curtis Beutler, Markus Bill
Supervision: Susan S. Hubbard, Kenneth H. Williams
Visualization: Matthias Sprenger
Writing – original draft: Matthias Sprenger
Writing – review & editing: Matthias Sprenger, Rosemary W. H. Carroll, James Dennedy-Frank, Erica R. Siirila-Woodburn, Michelle E. Newcomer, Susan S. Hubbard, Kenneth H. Williams

in the East River, Colorado to address how the partitioning of snow and rain into summer runoff and ET vary across headwater catchments of contrasting landscape characteristics and in response to meteorological variation.

2. Methods

2.1. Study Sites and Data

Our study took place in the East River Watershed (Figure 1) in the Upper Colorado River Basin (UCRB) (Hubbard et al., 2018). The lithology of the main stem East River Watershed is dominated by Cretaceous Mancos shale bedrock with Oligocene quartz monzonite and granodiorite laccoliths comprising many of the higher elevation peaks. At Coal Creek, the underlying bedrock is mainly composed of Cretaceous and Eocene sandstones, mudstones, and quartz monzonite and granodiorite intrusive rocks (Gaskill et al., 1991; Uhlemann et al., 2022). The climate in the region is defined as continental subarctic with long, cold winters and short, cool summers (Dfc, according to Koeppen-Geiger, Peel et al., 2007). Due to the large elevation gradient from 2,600 to 4,380 m a.s.l., meteorological conditions vary strongly within the catchments. Based on the two SNOTEL sites within the East River, Schofield at 3,261 m a.s.l. and Butte at 3,097 m a.s.l., the average daily air temperature ranges between −8.3°C in December and 11°C in June at the lower-elevation site with about 1.6°C colder temperatures at the high-elevation site (Carroll et al., 2018). Precipitation is dominated by snow, accounting for about 70% of precipitation at Schofield and 66% at Butte. However, annual average precipitation is almost double at the higher Schofield site (1,200 ± 233 mm/year) compared to the lower-elevation site Butte (670 ± 120 mm/year) SNOTEL site (Carroll et al., 2018).

Our study includes nine sub-catchments from the East River as defined in Figure 1. Catchment characteristics vary greatly in their size; average slope; aspect; average elevation; relief; drainage density; topographic wetness index; average tree cover derived from USGS Landfire raster maps (LANDFIRE, 2015); the catchment's share of montane, subalpine, upper subalpine, and alpine life zones as well as their share of Mancos shale or barren land (Table S1 in Supporting Information S1). Dominant forest cover in the study region is conifer (Spruce-Fir and Lodgepole Pine) and to lesser extent aspen forest (about 10% of area). With elevation, grass and forb cover increases, and above 3,700 m barren land, defined as rocky outcrops and sparse vegetation, dominates. The catchment areas range between 2.55 and 85 km^2. The dominant aspect for the western sub-catchments is east, while the eastern sub-catchments are primarily southwest. Average catchment elevation ranges between 3,148 and 3,513 m a.s.l. and the relief is between 904 and 1,362 m (Table S1 in Supporting Information S1).

We measured streamflow at each catchment outlet (Carroll & Willlams, 2019; Carroll et al., 2020) and filled gaps that occurred based on a machine learning approach described in the supplementary material (Text S1 in Supporting Information S1, Newcomer et al., 2022). Since water year 2015, we sampled the stream water through automatic samplers (Model 3,700; Teledyne ISCO, NE, USA) at the Pumphouse and Coal Creek locations at daily to fortnightly frequency and via manual sampling at the other catchment outflows on weekly to twice monthly frequency (Williams et al., 2020). Precipitation was sampled on event basis in the water years 2015 and 2016 and quantified as snow or rain (Figure 1, Carroll et al., 2021). To prevent fractionation prior to sample retrieval, bottles were pre-filled with 2-cm mineral oil to serve as a barrier to evaporation. All samples were filtered through 0.45-µm Polyvinylidene difluoride (PVDF) membrane filters (EMD Millipore Corp.) into 2-mL septa-capped glass vials and refrigerated until analysis. We measured the isotope ratios of water (^2H and ^{18}O) via off-axis integrated cavity output spectrometry (Picarro L2130-i or Los Gatos Research Liquid Water Isotope Analyzer) and report all isotope ratios in δ-notation relative to the Vienna Standard Mean Ocean Water. Precision of the analyses is 0.025 and 0.1‰ for $\delta^{18}O$ and δ^2H, respectively, and outliers of stream water samples with $\delta^{18}O > 11‰$ were discarded.

2.2. Analyses

2.2.1. Endmember Splitting and Mixing Analysis

Based on the $\delta^{18}O$ data in precipitation and streamflow, we applied endmember splitting and mixing analyses (Kirchner, 2019; Kirchner & Allen, 2020). We defined snow (P_S) and rain (P_R) as the two endmembers because of their distinct isotopic compositions with weighted averages of $\delta^{18}O_{PS} = -18.18$ ‰ and $\delta^{18}O_{PR} = -6.90$ ‰, respectively (Figure S1 in Supporting Information S1). We differentiated the temporal and catchment specific

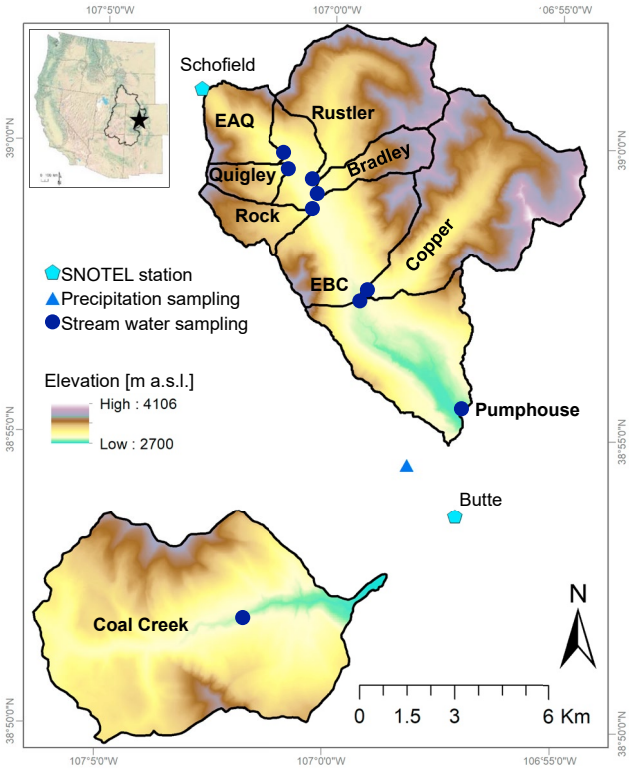

Figure 1. Location of stream water and precipitation sampling as well as the SNOTEL stations in the study area. Name, boundaries and elevation distribution of all nine catchments shown. Upper left insert shows the Upper Colorado Basin (black line) and the East River (star) within the western US. Longitude and latitude are provided at the ticks of the map frame.

variations in snow and rainfall based on air temperature variations, precipitation, and Airborne Snow Observatory snow depth estimates provided by Carroll, Deems, Sprenger, et al. (2022) to estimate P_S and P_R volumes for each of the nine catchments. Spatial variation of $\delta^{18}O$ was accounted for based on a isotope lapse rate of −0.16‰/100 m, derived from weekly sampling of snowfall along an elevation gradient (Carroll, Deems, Maxwell, et al., 2022). We separated the stream water during summer (July–September) and non-summer (October–June) periods as the two output endmembers, Q_S and Q_{nS}, respectively. With this definition, the snowmelt peak runoff occurred during Q_{nS}, while Q_S covered the hydrograph recession, including the monsoon season (Figures S2–S10 in Supporting Information S1). Precipitation isotope ratios were weighted by the respective precipitation sums, and the discharge isotope ratios were weighted by the flow volume at the sampling day.

We conducted the endmember splitting and mixing analyses for all available data from water-years 2015–2020, which when aggregated, approaches the long-term isotope mass balance. We also conducted the analyses for the individual years for all the catchments that had sufficient stream water isotope data available. For endmember mixing and splitting analyses, the water balance is assumed to be closed (Kirchner & Allen, 2020), because it implies that the catchment storage change is zero and that the ET sum is the difference between precipitation and catchment streamflow sums. For the inter-annual analyses this assumption might not be valid, so we focus our interpretation mostly on the long-term analyses. Losses to the regional groundwater system are small, as environmental tracer analyses revealed mean residence times of thousands of years (mean = 3200 years) for the groundwater close to the Pumphouse location in Figure 1 (Thiros et al., 2022). Hydrological modeling results further indicate that the interannual storage variability for the considered catchments were between 1987 and 2018 on average 0.04% ± 4.9% of the annual P (Carroll et al., 2019). All results are given with ± standard errors based on Gaussian error propagation as outlined by Kirchner and Allen (2020).

2.2.2. Statistical Analyses

As the catchment characteristics are highly cross-correlated (Figure S11 in Supporting Information S1), we applied a rotated principle component analysis to extract four components that represented the variation of the following catchment characteristics: share of alpine and montane area, respectively, drainage density, topographic wetness index, catchment area, share of Mancos shale in catchment, average elevation, relief, average slope, average aspect, and tree cover (Table S1 in Supporting Information S1). For each of the four relative components, we picked the one catchment character that correlated the most with the individual components (Figure S12 in Supporting Information S1) to be a representative predictor. With these four representative predictors, we performed a multiple linear regression (MLR) analysis and derived the Pearson correlation coefficient (r^2) and relative importance of each predictor to describe the spatial variance of endmember mixing and splitting results across the nine catchments.

3. Results: Snow and Rain Contributions to Summer Runoff and Evapotranspiration

3.1. Spatial Variability

Snow provided 85% of total precipitation between 2015 and 2020, and consequently our endmember mixing analyses revealed that across all catchments (average ± standard deviation) snow was the dominant water source for Q_{nS} (94 ± 3%), Q_S (90% ± 1%) and ET (74 ± 8%) (Table S2 in Supporting Information S1). Therefore, snowmelt was—relatively to the input volumes—overrepresented in Q and underrepresented in ET. Conversely, rainfall played a special role in sustaining ET fluxes during the summer. The fraction of rain and snow in Q_{nS}

and Q_S across the catchments was well explained by the MLR analyses ($r^2 = 0.78$, $p = 0.125$ and $r^2 = 0.74$, $p = 0.164$ respectively) with the average catchment aspect being the main driver (Figure 2a). In more westerly exposed catchments, Q_S and Q_{nS} typically contained less rain (Q_S from P_R, $r = -0.79$, $p = 0.01$ and Q_{nS} from P_R, $r = -0.88$, $p < 0.01$, respectively, Figures 2e and 2f). This relationship is due to a greater ET dominance at westerly exposed hillslopes, where summers are warmer and thus rain potentially evapotranspires shortly after it falls leading to less rainwater sourcing for streamflow in western facing catchments. The share of snow and rain in ET (ET from P_R) was generally more variable across the catchments. MLR described its variation moderately well ($r^2 = 0.63$, $p = 0.31$) with tree cover explaining 34% of the regression and aspect and drainage density explaining 27% and 24% of the variability respectively (Figure 2a). In general, there was a higher share of snow in ET (ET from P_S) in catchments with higher tree cover ($r = 0.53$, $p = 0.15$), which explains much of the inter-catchment variation of the endmember mixing results. Consequently, Q_{nS} and Q_S had a lower share of snow with increasing tree cover. Neither the catchment's drainage density nor size was a good predictor of the snow and rain contributions to the outflows.

Our endmember splitting results show that most rain was to partition into ET (67% ± 15%, P_R to ET), while only a small fraction (8% ± 4%) of the summer rainfall became Q_S (P_R to Q_S), and that 24% ± 13% of rain left the catchments via Q_{nS} (P_R to Q_{nS}) (Table S2 in Supporting Information S1). In contrast, only 33% ± 12% of snow ended up as ET (P_S to ET) while most of the snow became Q_{nS} (53 ± 9%, P_S to Q_{nS}) and to lesser extent Q_S (13% ± 6%, P_S to Q_S).

Vegetation cover provided a primary control on the differences in endmember splitting across the catchments. Our relative importance results show that tree cover accounted for 78% of the explained variance in a MLR. Increasing tree cover decreased the share of rainfall that partitions to Q_S (Figures 2a and 2b). The share of rain becoming Q_{nS} was mainly determined by the catchment aspect and the catchment size, but the predictive power of the MLR model was low ($r^2 = 0.33$, $p = 0.74$), which makes interpretations uncertain. Aspect was also the most important factor for the regression to explain the variation in the fraction of rainfall becoming ET. However, the coefficient of determination was low and the relationship not significant ($r^2 = 0.28$, $p = 0.81$) (Figure 2a).

The multiple regression models for the spatial variation of the snow endmember splitting showed much better coefficients of variation than for the rainfall splitting. The share of snow that became Q_S was well described ($r^2 = 0.93$, $p = 0.02$) with tree cover (53%) and average aspect (33%) as the two important predictors. With increasing tree cover, snow was less likely to become Q_S ($r = -0.82$, $p = 0.01$, Figure 2c), because more snow ended up in ET ($r = 0.72$, $p = 0.03$, Figure 2d). Therefore, tree cover was the most important predictor (69%) in the regression model explaining the variability of snow becoming ET. Aspect played a secondary role for the snow contributions to Q_{nS} ($r = 0.68$, $p = 0.04$, Figure 2g). Drainage density explained some of the variability in snowfall becoming Q_{nS}, however, this correlation was weak and not statistically significant.

In addition to the catchment characteristics, hydrometeorological variations across the catchments also impacted the endmember mixing and splitting results. We found that as ET magnitude increases, a greater percentage of that ET (significant for 2015, 2016, 2019, 2020, Figure 3a) and thus more ET flux volume (Figure S15a in Supporting Information S1) was sourced from snow. We explain this result by belowground snowmelt storage subsiding to supporting ET during water limited conditions in the summer that occur in subalpine and montane elevations (Carroll et al., 2020). This dependency of ET on snowmelt contributions was further supported by the observed trend that in catchments with more snowfall, more of the snow became ET during low-snow years (2015, 2016, 2018, Figure 3b). Notably, ET volume estimates that were based on the water balance did not correlate with P, P_S, nor P_R sums, but years with relatively lower ET sums were characterized by higher Q (Figure S16 in Supporting Information S1).

In general, higher ET in catchments—due to lower measured Q—led to a greater percentage of snow becoming ET (Figure 3g), and less snow ending up in Q_{nS} (Figure 3e) which underlies the importance of snow sources and spatial variability for ET fluxes. There was no correlation between the rainfall contributions to ET and inter-annual variation of ET sums, which shows that most of the rainfall was generally—independently of the evaporative demand—becoming ET. The importance of monsoon rains in sustaining Q_S was also documented: catchments with higher rainfall sums not only resulted in higher Q_S, but also resulted in more snow becoming Q_S (Figure 3d and Figure S15d in Supporting Information S1) which indicated that snow stored in the subsurface was

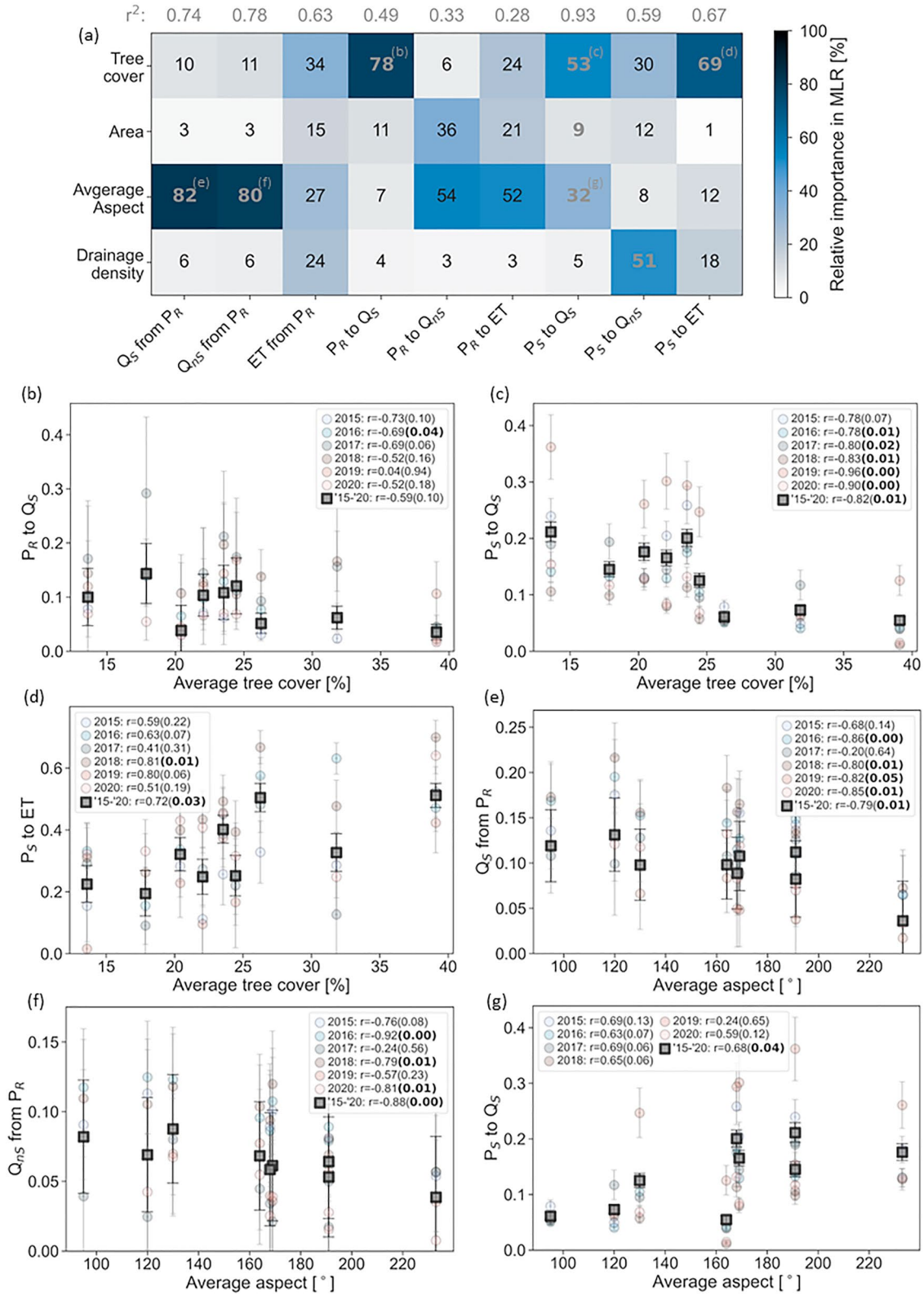
r²: 0.74 0.78 0.63 0.49 0.33 0.28 0.93 0.59 0.67
(a)
Tree cover
Area
Avgerage Aspect
Drainage density
10 11 34 78(b) 6 24 53(c) 30 69(d)
3 3 15 11 36 21 9 12 1
82(e) 80(f) 27 7 54 52 32(g) 8 12
6 6 24 4 3 3 5 51 18
Qs from PR
QnS from PR
ET from PR
PR to QS
PR to QnS
PR to ET
PS to QS
PS to QnS
PS to ET
Relative importance in MLR [%]
(b) PR to QS
(c) PS to QS
(d) PS to ET
(e) QS from PR
(f) QnS from PR
(g) PS to QS
Average tree cover [%]
Average aspect [°]

Figure 2.

mobilized by summer rainfall and thus contributing to summer streamflow. Outside of summers, more of Q_{nS} was sourced by snow as flow increased (Figure 3f).

3.2. Temporal Variability

The spatial relationships between endmember mixing and splitting results and catchment characteristics were relatively constant in time (see half-transparent circles in Figures 2b–2g). However, there are inter-annual dynamics in the partitioning that stem from the hydrometeorological conditions. For example, in years with higher P_R, more ET was sourced from rain ($r = 0.99$, $p < 0.01$, Figure 3c), which was strengthened by a higher P_R/P_S ratio in 2015 (see Figure S14 in Supporting Information S1 for water balance volumes for each year and catchment). Endmember splitting further showed that there was also a trend of a higher share of rainfall becoming ET as rainfall and ET volumes increased ($r = 0.63$, $p = 0.18$ and $r = 0.73$, $p = 0.10$, respectively), leaving a lower share of rain to support streamflow. Wetter years with higher Q_{nS} resulted in more snow becoming Q_{nS} (Figure 3f and Figure S15f in Supporting Information S1) and a lower fraction of snow (Figure 3h) and less snow volume (Figure S15h in Supporting Information S1) ended up as ET.

Not surprisingly, there was a trend toward more snow in both Q_S and Q_{nS} ($r = 0.77$, $p = 0.08$ and $r = 0.75$, $p = 0.09$, respectively) for years with higher SWE_{max}, but the splitting of snow into ET and Q was independent of the annual SWE_{max}.

4. Discussion

Similar to the initial endmember splitting and mixing work by Kirchner and Allen (2020) for the humid Watershed 3 at Hubbard Brook Experimental Forest, our analyses shows that inter-seasonal water storage is an integral part of storage and release of water in headwater mountainous catchments. However, the snow dominance of the water balance in the UCRB and the resulting hydrograph led to different precipitation partitioning dynamics than for Hubbard Brook.

Our multi-catchment approach permitted inference of controls on the spatial variability in precipitation partitioning in mountainous regions. We found that aspect and tree cover were the main driver of the spatial variability. More SW exposed catchments had a higher share of snow in their streamflow, which cannot be explained by spatial variation in snow, because SW exposed catchments had lower snowpack volumes than the NE exposed ones (Carroll, Deems, Sprenger, et al., 2022). Thus, the influence of aspect on the snowmelt timing and the consequences for the runoff generation and the timing of the transpiration onset seems to govern the partitioning. As more of the snowmelt happens earlier in catchments with more hillslopes exposed to the SW, the snowmelt drains toward the stream and groundwater and is therefore less likely to get evapotranspired (Barnhart et al., 2016; Jeton et al., 1996; Molotch et al., 2009). By the time snowmelt happens at NE exposed hillslopes ET rates are already higher, which then changes the partitioning of the snow toward higher losses via ET. The variability in rain and snow partitioning has implications for critical watershed functions, such as water delivery, drought resilience, and nitrogen export, and our results help to explain potential sources and mechanisms of these observed functions (Newcomer et al., 2021; Wainwright et al., 2022).

Our tracer based results for head-water catchments indicate that 90% of runoff is sourced by snow, which is the upper limit of the water balance based estimates for various locations across the western US (Li et al., 2017). That our results are at the upper limit is due to the relatively high P_S/P_R ratio in our high-elevation study area compared to other regions in the western US (Li et al., 2017). Specifically for the East River, our findings corroborate hydrologic modeling results that showed that most rain gets evapotranspired, and little rain becomes runoff to the East River (Carroll et al., 2020). Our estimate of ~7% of total Q stemming from rain for the East River at Pumphouse is within the range of modeled estimates (~10%, Carroll et al., 2020). Our findings support ET source water estimates from particle tracking simulations, which indicated that ET of a forested hillslope in the East River catchment was to large parts sourced by snowmelt (Maxwell et al., 2019). Their simulations

Figure 2. (a) Relative importance of a multiple linear regression (MLR) model to explain variability of endmember mixing and splitting results. Bold gray numbers indicate regression parameters with p-values < 0.1. The coefficient of determination (r^2) of the regression models explaining the variation of the endmember mixing and splitting results across the catchments are shown in gray above each column. The individual relationships for significant parameters of high relative importance are shown in inserts (b–g) and Pearson's correlation coefficient and p-values are provided in the legends for each year and the long-term analyses 2015–2020. Error bars represent standard errors based on Gaussian error propagation.

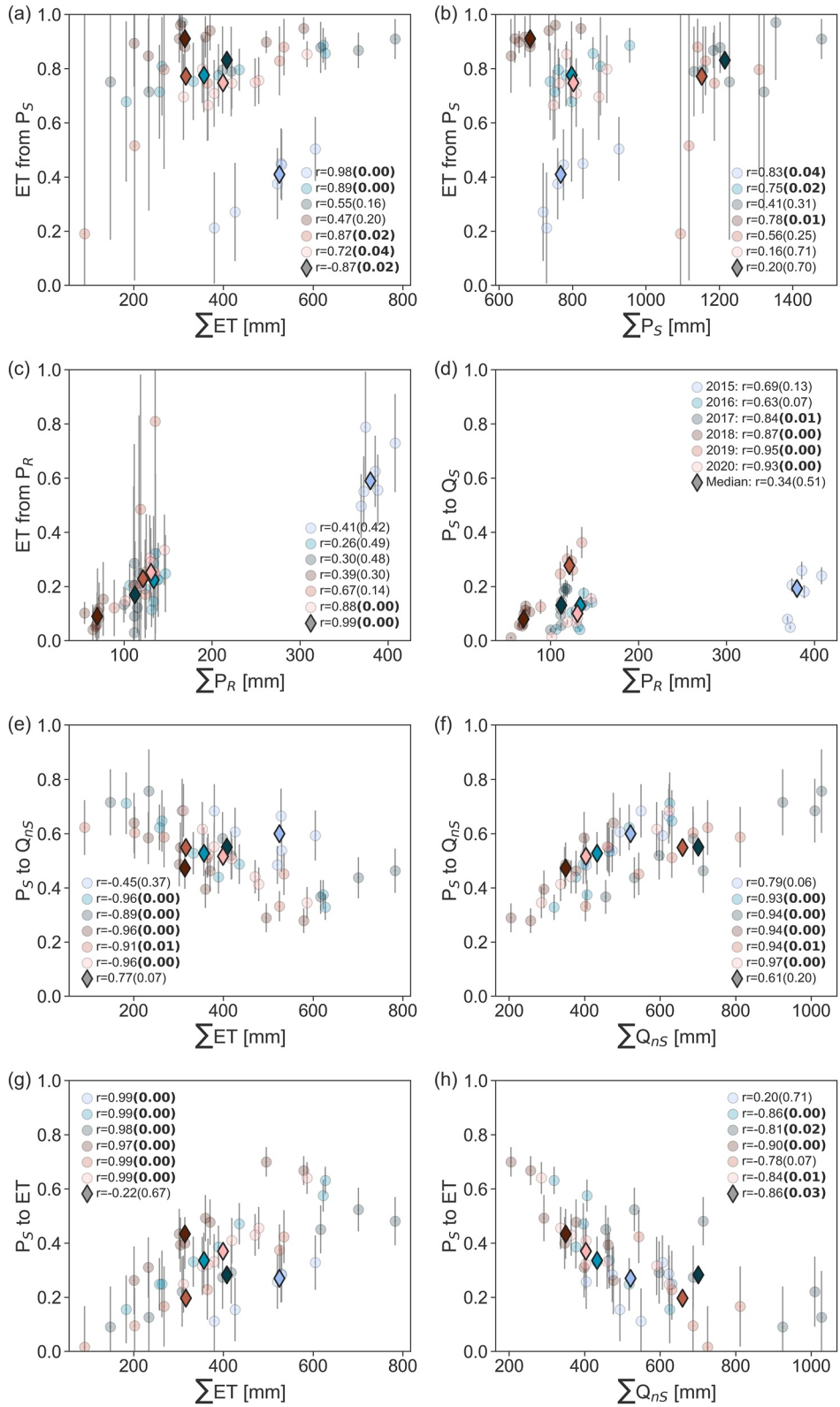
(a)
ET from P_S
$\sum$ET [mm]
r=0.98(0.00)
r=0.89(0.00)
r=0.55(0.16)
r=0.47(0.20)
r=0.87(0.02)
r=0.72(0.04)
r=-0.87(0.02)
(b)
ET from P_S
$\sum P_S$ [mm]
r=0.83(0.04)
r=0.75(0.02)
r=0.41(0.31)
r=0.78(0.01)
r=0.56(0.25)
r=0.16(0.71)
r=0.20(0.70)
(c)
ET from P_R
$\sum P_R$ [mm]
r=0.41(0.42)
r=0.26(0.49)
r=0.30(0.48)
r=0.39(0.30)
r=0.67(0.14)
r=0.88(0.00)
r=0.99(0.00)
(d)
P_S to Q_S
$\sum P_R$ [mm]
2015: r=0.69(0.13)
2016: r=0.63(0.07)
2017: r=0.84(0.01)
2018: r=0.87(0.00)
2019: r=0.95(0.00)
2020: r=0.93(0.00)
Median: r=0.34(0.51)
(e)
P_S to Q_{nS}
$\sum$ET [mm]
r=-0.45(0.37)
r=-0.96(0.00)
r=-0.89(0.00)
r=-0.96(0.00)
r=-0.91(0.01)
r=-0.96(0.00)
r=0.77(0.07)
(f)
P_S to Q_{nS}
$\sum Q_{nS}$ [mm]
r=0.79(0.06)
r=0.93(0.00)
r=0.94(0.00)
r=0.94(0.00)
r=0.94(0.01)
r=0.97(0.00)
r=0.61(0.20)
(g)
P_S to ET
$\sum$ET [mm]
r=0.99(0.00)
r=0.99(0.00)
r=0.98(0.00)
r=0.97(0.00)
r=0.99(0.00)
r=0.99(0.00)
r=-0.22(0.67)
(h)
P_S to ET
$\sum Q_{nS}$ [mm]
r=0.20(0.71)
r=-0.86(0.00)
r=-0.81(0.02)
r=-0.90(0.00)
r=-0.78(0.07)
r=-0.84(0.01)
r=-0.86(0.03)

Figure 3.

indicated that between Mid-June to September, rainfall became a more important ET source, which aligns with our finding that most of the rainfall is evapotranspired. The importance of snow for transpiration is further supported by isotope-based plot-scale ecohydrological studies in the East River (Berkelhammer et al., 2020) and across Switzerland (Allen et al., 2019). Berkelhammer et al. (2020) showed that rain becomes a more important plant water source as it infiltrates into the shallow soil layers and is subsequently taken up by trees in the later growing season. While these isotope studies and tracer-based modeling work (Brinkmann et al., 2018; Sprenger et al., 2018) at the plot-scale indicated that trees take up relatively old (e.g., snowmelt) water, our catchment-wide isotope water balances revealed that these ecohydrological processes are generally relevant for storage and release of water at the catchment scale. Our findings underlie both the importance of snow water uptake by plants and also the quick turnover time of rainfall becoming ET, as two-thirds of the rainfall was evapotranspired according to our endmember splitting analyses.

Due to ecohydrological feedbacks between subsurface water storage and root water uptake, vegetation cover played a crucial role in our study to explain partitioning of snow and rainfall into Q and ET. We infer that with higher tree cover, the rooting system will be more efficient in extracting potentially deeper soil layers where snowmelt is being stored during the summer, sustaining the summertime evaporative demand. Carroll et al. (2018) found that the groundwater fraction in the streamflow decreases with tree cover across East River catchments. Since snow is the main source of groundwater recharge in the East River, our results support the finding that snow contributions to runoff decreases with tree cover. Our multi-year analysis shows that this relationship between tree cover and runoff processes is relatively constant in time. Consequences of a low-to-no-snow future for these processes would depend on the rainfall being able to compensate the snow water loss or not. An earlier onset of the vegetation period and earlier loss to ET that would accompany a snowpack reduction and result in pronounced ecohydrological feedbacks toward a higher share of precipitation partitioning to ET rather Q compared to the current conditions. Such changes would pose a potential for drought stress for plants (Harpold, 2016), higher risk of fires, and changes to water and chemical exports that are currently adapted to inter-seasonal water storage (Newcomer et al., 2021).

The higher share of snow in ET with increased ET sum that we observed can explain the "drought-paradox" (Teuling et al., 2013), that ET can increase during periods with lack of precipitation. Since ET is sourced in large part (60%–80%) from snow in the UCRB, a reduced monsoon rainfall will have relatively little impact on ET rates. Conversely, greater monsoon rains during summer may result in a higher fraction and flux volume (see 2015 volumes in Figure S14 of Supporting Information S1) of P_R partitioning to ET, which lowers snow water losses to the atmosphere. As a result, snowmelt is more likely to become discharge as reflected in an increased partitioning to Q_S (Figure 3d). However, an increased ET flux leads to a higher share of snow in ET, which can cause a strong water deficiency in a warmer low-snow to no-snow future with increased ET demand (Milly & Dunne, 2020; Woodburn et al., 2021). The increase in ET due to tree cover extension in warming mountain ecosystems might be limited by water availability, though. This would result in an increased catchment runoff due to higher snowmelt infiltration in forested areas (e.g., due to snow wind-scour, Barnhart et al., 2021).

Our endmember mixing and splitting results highlight that climate projections will need to account for such ecohydrological interactions between shifts in snow volumes, the timing of melt and the resulting soil and bedrock moisture dynamics that impact plant water use during climatic extremes (e.g., Mastrotheodoros et al., 2020). Despite uncertainties associated with the spatial and temporal variability in snow and rain volumes and stable isotope ratios (Carroll, Deems, Sprenger, et al., 2022), these two endmembers are isotopically strongly dissimilar, and thus, the observed patterns have been consistent both in space (across the catchments) and in time (individual years and long-term mass balance). Endmember mixing and splitting has therefore shown to be highly informative for catchment scale processes, which helps benchmark hydrological models and assess sources and mechanisms for changing watershed conditions.

Figure 3. (a–c) Endmember mixing and (d–h) endmember splitting results as a function of hydrometric data: annual sums of evapotranspiration (ET), snowfall (P_S), rainfall (P_R), and non-summer streamflow (Q_{nS}). Shown are results from individual catchments and years (circles and color coded, see legend in subplot d) as well as median values across all catchments for individual years (diamonds). Correlation coefficients (r) and p-values are shown in brackets in the legends, while bold font indicates significant correlations ($p < 0.05$). Circles represent variability across catchments for individual years and diamonds represent variability between different years averaged over the catchments. Error bars represent standard errors based on Gaussian error propagation. Please see Figure S15 in Supporting Information S1 for the same plots with flux volumes on the y-axis.

5. Conclusion

Our results show how stable isotopes of water can inform our perspective of catchment scale hydrological partitioning and mass balance components in snow-dominated mountainous regions. Observed partitioning of snow and rain into either ET or summer and non-summer Q highlighted the importance of snowmelt contributions to catchment storage that sustain not only the seasonal streamflow, but also evaporative demand in the vegetated headwaters. Variability across the nine catchments showed the influence of vegetation on mixing and splitting, as higher tree cover resulted in higher snow water loss to the atmosphere and less snow contributing to streamflow. Two-thirds of the summer rainfall was evapotranspired, while only ∼10% of the summer streamflow was from rainfall. We therefore conclude that in a future low-snow mountain environment, the evaporative demand of the forested catchments will only be met with a pronounced increase in rainfall to overcome water scarcity for ecosystem and anthropogenic use. Our catchment scale isotope mass balance work can help upscale plot-scale observations and test hydrological models, which will improve mechanistic process representation of rain/snow partitioning under future climate regimes.

Conflict of Interest

The authors declare no conflicts of interest relevant to this study.

Data Availability Statement

The endmember mixing and splitting code (Kirchner, 2019) is available on EnviDat and the data on streamflow (Carroll et al., 2020; Newcomer et al., 2022) and stable isotope data (Carroll et al., 2021; Williams et al., 2020) are freely and publicly available online on the DOE ESS-DIVE data repository as cited.

Acknowledgments
This work was supported by the US Department of Energy Office of Science under contract DE-AC02-05CH11231 as part of Lawrence Berkeley National Laboratory Watershed Function Science Focus Area. We would like to express appreciation to the Rocky Mountain Biological Laboratory for handling US Forest Service permitting.

References

Allen, S. T., Kirchner, J. W., Braun, S., Siegwolf, R. T. W., & Goldsmith, G. R. (2019). Seasonal origins of soil water used by trees. *Hydrology and Earth System Sciences*, *23*(2), 1199–1210. https://doi.org/10.5194/hess-23-1199-2019

Barnhart, T. B., Molotch, N. P., Livneh, B., Harpold, A. A., Knowles, J. F., & Schneider, D. (2016). Snowmelt rate dictates streamflow. *Geophysical Research Letters*, *43*(15), 8006–8016. https://doi.org/10.1002/2016GL069690

Barnhart, T. B., Vukomanovic, J., Bourgeron, P., & Molotch, N. (2021). Future land cover and climate may drive decreases in snow wind-scour and transpiration, increasing streamflow at a Colorado, USA headwater catchment. *Hydrological Processes*, *35*(11), e14416. https://doi.org/10.1002/hyp.14416

Berkelhammer, M., Still, C. J., Ritter, F., Winnick, M., Anderson, L., Carroll, R., et al. (2020). Persistence and plasticity in conifer water-use strategies. *Journal of Geophysical Research: Biogeosciences*, *125*(2), e2018JG004845. https://doi.org/10.1029/2018JG004845

Brinkmann, N., Seeger, S., Weiler, M., Buchmann, N., Eugster, W., & Kahmen, A. (2018). Employing stable isotopes to determine the residence times of soil water and the temporal origin of water taken up by Fagus sylvatica and Picea abies in a temperate forest. *New Phytologist*, *219*(4), 1300–1313. https://doi.org/10.1111/nph.15255

Carroll, R. W. H., Bearup, L. A., Brown, W., Dong, W., Bill, M., & Willlams, K. H. (2018). Factors controlling seasonal groundwater and solute flux from snow-dominated basins. *Hydrological Processes*, *32*(14), 2187–2202. https://doi.org/10.1002/hyp.13151

Carroll, R. W. H., Brown, W., Newman, A., Beutler, C., & Williams, K. H. (2021). *East River watershed stable water isotope data in precipitation, snowpack and snowmelt 2016–2020*. ESS-DIVE Repository. https://doi.org/10.15485/1824223

Carroll, R. W. H., Deems, J., Maxwell, R., Sprenger, M., Brown, W., Newman, A., et al. (2022). Variability in observed stable water isotopes in snowpack across a mountainous watershed in Colorado. *Hydrological Processes*.

Carroll, R. W. H., Deems, J., Sprenger, M., Maxwell, R., Brown, W., Newman, A., et al. (2022). Modeling snow dynamics and stable water isotopes across mountain landscapes. *Earth and Space Science Open Archive*. https://doi.org/10.1002/essoar.10510911.1

Carroll, R. W. H., Deems, J. S., Niswonger, R., Schumer, R., & Williams, K. H. (2019). The importance of interflow to groundwater recharge in a snowmelt-dominated headwater basin. *Geophysical Research Letters*, *46*(11), 5899–5908. https://doi.org/10.1029/2019GL082447

Carroll, R. W. H., Gochis, D., & Williams, K. H. (2020). Efficiency of the summer monsoon in generating streamflow within a snow-dominated headwater basin of the Colorado River. *Geophysical Research Letters*, *47*(23), e2020GL090856. https://doi.org/10.1029/2020GL090856

Carroll, R. W. H., Newman, A., Beutler, C., & Williams, K. H. (2020). *Stream discharge data collected within the East River, Colorado for the Lawrence Berkeley National Laboratory Watershed Function Science Focus Area (water year 2019–2020, present)*. ESS-DIVE Repository. https://doi.org/10.15485/1779721

Carroll, R. W. H., & Willlams, K. H. (2019). Discharge data collected within the East River for the LBNL Watershed Function Science Focus Area (water years 2015–2018). *Watershed Functionality Scientific Focus Area*. https://doi.org/10.21952/WTR/1495380

Gaskill, D. L., Mutschler, F. E., & Kramer, J. H. (1991). Geologic map of the Gothic quadrangle.

Harpold, A. A. (2016). Diverging sensitivity of soil water stress to changing snowmelt timing in the Western U.S. *Advances in Water Resources*, *92*, 116–129. https://doi.org/10.1016/j.advwatres.2016.03.017

Hock, R., Rasul, G., Adler, C., Cáceres, B., Gruber, S., Hirabayashi, Y., et al. (2019). High mountain areas. In H.-O. Pörtner, D. C. Roberts, V. Masson-Delmotte, P. Zhai, M. Tignor, E. Poloczanska, et al. (Eds.), *IPCC Special Report on the Ocean and Cryosphere in a Changing Climate*.

Hubbard, S. S., Williams, K. H., Agarwal, D., Banfield, J., Beller, H., Bouskill, N., et al. (2018). The East River, Colorado, Watershed: A mountainous community testbed for improving predictive understanding of multiscale hydrological–biogeochemical dynamics. *Vadose Zone Journal*, *17*(1), 180061–25. https://doi.org/10.2136/vzj2018.03.0061

Ikeda, K., Rasmussen, R., Liu, C., Newman, A., Chen, F., Barlage, M., et al. (2021). Snowfall and snowpack in the Western U.S. as captured by convection permitting climate simulations: Current climate and pseudo global warming future climate. *Climate Dynamics*, *57*(7), 2191–2215. https://doi.org/10.1007/s00382-021-05805-w

Immerzeel, W. W., Lutz, A. F., Andrade, M., Bahl, A., Biemans, H., Bolch, T., et al. (2020). Importance and vulnerability of the world's water towers. *Nature*, *577*(7790), 364–369. https://doi.org/10.1038/s41586-019-1822-y

Jeton, A. E., Dettinger, M. D., & Smith, J. L. (1996). *Water-Resources Investigations Report 95-4260: Potential effects of climate change on streamflow, eastern and western slopes of the Sierra Nevada, California and Nevada*. USGS.

Kirchner, J. W. (2019). EndSplit [Dataset]. EnviDat. https://doi.org/10.16904/envidat.91

Kirchner, J. W., & Allen, S. T. (2020). Seasonal partitioning of precipitation between streamflow and evapotranspiration, inferred from end-member splitting analysis. *Hydrology and Earth System Sciences*, *24*(1), 17–39. https://doi.org/10.5194/hess-24-17-2020

LANDFIRE. (2015). Existing vegetation type and cover layers. Retrieved from http://landfire.cr.usgs.gov/viewer/

Li, D., Wrzesien, M. L., Durand, M., Adam, J., & Lettenmaier, D. P. (2017). How much runoff originates as snow in the western United States, and how will that change in the future? *Geophysical Research Letters*, *44*(12), 6163–6172. https://doi.org/10.1002/2017GL073551

Mastrotheodoros, T., Pappas, C., Molnar, P., Burlando, P., Manoli, G., Parajka, J., et al. (2020). More green and less blue water in the Alps during warmer summers. *Nature Climate Change*, *10*(2), 155–161. https://doi.org/10.1038/s41558-019-0676-5

Maxwell, R. M., Condon, L. E., Danesh-Yazdi, M., & Bearup, L. A. (2019). Exploring source water mixing and transient residence time distributions of outflow and evapotranspiration with an integrated hydrologic model and Lagrangian particle tracking approach. *Ecohydrology*, *12*(1), e2042. https://doi.org/10.1002/eco.2042

Milly, P. C. D., Dunne, K. A., Yu, Z., Kong, P., Sefik, E., Xu, H., et al. (2020). Colorado River flow dwindles as warming-driven loss of reflective snow energizes evaporation. *Science*, *367*(6483), 1252–1255. https://doi.org/10.1126/science.aax0194

Molotch, N. P., Brooks, P. D., Burns, S. P., Litvak, M., Monson, R. K., Mcconnell, J. R., & Musselman, K. (2009). Ecohydrological controls on snowmelt partitioning in mixed-conifer sub-alpine forests. *Ecohydrology*, *2*, 129–142. https://doi.org/10.1002/eco.48

Musselman, K. N., Addor, N., Vano, J. A., & Molotch, N. P. (2021). Winter melt trends portend widespread declines in snow water resources. *Nature Climate Change*, *11*(5), 418–424. https://doi.org/10.1038/s41558-021-01014-9

Newcomer, M. E., Bouskill, N. J., Wainwright, H., Maavara, T., Arora, B., Siirila-Woodburn, E. R., et al. (2021). Hysteresis patterns of watershed nitrogen retention and loss over the past 50 years in United States hydrological basins global biogeochemical cycles. *Global Biogeochemical Cycles*, *35*(4), 1–28. https://doi.org/10.1029/2020GB006777

Newcomer, M. E., Williams, K. W., & Carroll, R. W. H. (2022). *Machine learning assisted gap-filled discharge data for the East River Community Watershed for water years 2014–2021*. ESS-DIVE Repository. https://doi.org/10.15485/1868939

Peel, M. C., Finlayson, B. L., & Mcmahon, T. A. (2007). Updated world map of the Koeppen-Geiger climate classification. *Hydrology and Earth System Sciences*, *11*(5), 1633–1644. https://doi.org/10.5194/hess-11-1633-2007

Sprenger, M., Tetzlaff, D., Buttle, J., Laudon, H., & Soulsby, C. (2018). Water ages in the critical zone of long-term experimental sites in northern latitudes. *Hydrology and Earth System Sciences*, *22*(7), 3965–3981. https://doi.org/10.5194/hess-22-3965-2018

Teuling, A. J., Van Loon, A. F., Seneviratne, S. I., Lehner, I., Aubinet, M., Heinesch, B., et al. (2013). Evapotranspiration amplifies European summer drought. *Geophysical Research Letters*, *40*(10), 2071–2075. https://doi.org/10.1002/grl.50495

Thiros, N. E., Gardner, W. P., Siirila-Woodburn, E. R., & Frank, J. P. D. (2022). Constraining bedrock groundwater residence times in mountain systems with environmental tracer observations and Bayesian uncertainty quantification. In *Frontiers in Hydrology Meeting*. Retrieved from https://agu.confex.com/agu/hydrology22/meetingapp.cgi/Paper/1035206

Uhlemann, S., Dafflon, B., Wainwright, H. M., Williams, K. H., Minsley, B., Zamudio, K., et al. (2022). Surface parameters and bedrock properties covary across a mountainous watershed: Insights from machine learning and geophysics. *Science Advances*, *8*(12), 1–16. https://doi.org/10.1126/sciadv.abj2479

Wainwright, H. M., Uhlemann, S., Franklin, M., Falco, N., Bouskill, N. J., Newcomer, M. E., et al. (2022). Watershed zonation through hillslope clustering for tractably quantifying above- and below-ground watershed heterogeneity and functions. *Hydrology and Earth System Sciences*, *26*(2), 429–444. https://doi.org/10.5194/hess-26-429-2022

Williams, K. H., Beutler, C. A., Bill, M., Brown, W., Newman, A. W., & Versteeg, R. (2020). *Stable water isotope data for the East River Watershed, Colorado*. *Watershed Function SFA*. ESS-DIVE Repository. https://doi.org/10.15485/1668053

Woodburn, E. R. S., Rhoades, A. M., Szinai, J., Tague, C., Nico, P. S., & Huning, L. S. (2021). A low-to-no snow future and its impacts on water resources in the western United States. *Nature Reviews Earth & Environment*, *2*(11), 800–819. https://doi.org/10.1038/s43017-021-00219-y

References From the Supporting Information

Breiman, L. (2001). Random forests. *Machine Learning*, *45*(1), 5–32. https://doi.org/10.1023/A:1010933404324

Dwivedi, D., Mital, U., Faybishenko, B., Dafflon, B., Varadharajan, C., Agarwal, D., et al. (2022). Imputation of contiguous gaps and extremes of subhourly groundwater time series using random forests. *Journal of Machine Learning for Modeling and Computing*, *3*(2), 1–22. https://doi.org/10.1615/JMachLearnModelComput.2021038774

Hirsch, R. M., & De Cicco, L. (2015). User guide to Exploration and Graphics for RivEr Trends (EGRET) and dataRetrieval: R packages for hydrologic data (version 2.0, February 2015). https://doi.org/10.3133/tm4A10

Jain, P., Coogan, S. C. P., Subramanian, S. G., Crowley, M., Taylor, S., & Flannigan, M. D. (2020). A review of machine learning applications in wildfire science and management. *Environmental Reviews*, *28*(4), 478–505. https://doi.org/10.1139/er-2020-0019

Liaw, A., & Wiener, M. (2018). *Breiman and Cutler's random forests for classification and regression*. CRAN. Retrieved from https://www.stat.berkeley.edu/~breiman/RandomForests/

Shortridge, J. E., Guikema, S. D., & Zaitchik, B. F. (2016). Machine learning methods for empirical streamflow simulation: A comparison of model accuracy, interpretability, and uncertainty in seasonal watersheds. *Hydrology and Earth System Sciences*, *20*(7), 2611–2628. https://doi.org/10.5194/hess-20-2611-2016

USGS. (2022). National Water Information System: Web interface. Retrieved from https://waterdata.usgs.gov/nwis